Draft version October 5, 2010
Preprint typeset using LaTeX style emulateapj v. 03/07/07

A UNIFIED THEORY FOR THE EFFECTS OF STELLAR PERTURBATIONS AND GALACTIC TIDES ON OORT CLOUD COMETS

Benjamin F. Collins[1] and Re'em Sari[1,2]

Draft version October 5, 2010

ABSTRACT

We examine the effects of passing field stars on the angular momentum of a nearly radial orbit of an Oort cloud comet bound to the Sun. We derive the probability density function (PDF) of the change in angular momentum from one stellar encounter, assuming a uniform and isotropic field of perturbers. We show that the total angular momentum follows a Lévy flight, and determine its distribution function. If there is an asymmetry in the directional distribution of perturber velocities, the marginal probability distribution of each component of the angular momentum vector can be different. The constant torque attributed to Galactic tides arises from a non-cancellation of perturbations with an impact parameter of order the semimajor axis of the comet. When the close encounters are rare, the angular momentum is best modeled by the stochastic growth of stellar encounters. If trajectories passing between the comet and sun occur frequently, the angular momentum exhibits the coherent growth attributed to the Galactic tides.

Subject headings: comets: general — Oort Cloud — solar system: formation

1. INTRODUCTION

In the same work as he proposed the existence of a large reservoir of comets in the outskirts of the solar system, Oort (1950) suggested a two-stage process for the creation of such a cloud. First, perturbations from the planets increase the semimajor axes of nearby smaller objects. These interactions leave the periapses of the small bodies in the planetary region, but will eventually deliver enough energy to eject them from the solar system. The second stage of Oort cloud formation requires that perturbations external to the solar system deliver angular momentum to the comets. This raises their periapses out of the realm of planetary influence and saves them from eventual ejection. Further perturbations are necessary to lower their periapses again so that they can return to the planetary region and be observed from Earth.

Oort's original suggestion for both the circularization and delivery mechanisms is the influence of other stars in the Galaxy as they encounter the solar system. Each star that passes the solar system delivers a small kick to each comet that depends on the mass of the star, its velocity, and its distance of closest approach. Heisler & Tremaine (1986) explored the effects of a large scale planar symmetry in the swarm of stellar perturbers to find a smooth torque similar in magnitude to or even dominant over the stochastic stellar perturbations. This effect is known as the "Galactic tidal torque," since it can be attributed to the gradient of the average potential of the Galactic disk. Several groups have used numerical simulations to investigate the formation of the Oort cloud from a combination of stellar perturbations and Galactic tides (Duncan et al. 1987; Dones et al. 2004); in all cases the two effects have been implemented separately.

Recent studies have provided analytic solutions to several other stochastic scattering problems that arise in orbital dynamics and planet formation (Collins & Sari 2006; Collins et al. 2007). Collins & Sari (2008) investigated the evolution of an initially circular orbit interacting impulsively with unbound perturbers. They showed that the probability per unit time of perturbing a circular orbit to an eccentricity of order e is proportional to e^{-1}. This power law is enough to determine that the eccentricity of the binary diffuses as a Lévy process, and the scale of the distribution grows linearly with time (Shlesinger et al. 1995). Such evolution is fast compared to the common Brownian motion-type diffusion where the distribution evolves as only the square-root of time.

In this work, we apply the framework developed for perturbations around nearly circular orbits in Collins & Sari (2008), hereafter CS08, to the case of perturbations around nearly radial orbits. Section 2 presents the effects of a single stellar passage on a zero angular momentum comet. In Section 3 we derive and solve the Boltzmann equation that describes the accumulation of the changes in angular momentum from an isotropic distribution of perturbers. Section 4 describes the perturbations that arise from an anisotropic velocity distribution, and explains the connection between the effects of stellar encounters and the tidal force from the Galactic potential. Section 5 summarizes our conclusions.

2. A SINGLE STELLAR PASSAGE

In this section we discuss the change in angular momentum, eccentricity, and periapse of a comet on a nearly radial orbit. We call the central body of the system the "sun." We denote the position of the comet as $\mathbf{r}_b(t)$, and its velocity

Electronic address: bfc@tapir.caltech.edu
[1] California Institute of Technology, MC 130-33, Pasadena, CA 91125
[2] Racah Institute of Physics, Hebrew University, Jerusalem 91904, Israel

$\mathbf{v}_b(t)$. We write the magnitude of $\mathbf{r}_b(t)$ as $r_b(t) = |\mathbf{r}_b(t)|$, and the unit vector as $\hat{r}_b(t) = \mathbf{r}_b(t)/r_b(t)$. Since a radial orbit is by definition a straight line, $\hat{r}_b(t)$ is constant in time. Furthermore, the direction of the velocity, $\hat{v}_b(t)$, is either aligned or anti-aligned with $\hat{r}_b$. The orbital energy per unit mass of the comet, $\mathcal{E}$, sets the semimajor axis, a, and the orbital period, $T_{\rm orb}$. The angular momentum vector, $\mathbf{J}$ is zero, and the eccentricity vector is then given by $\mathbf{e} = \mathbf{v}_b \times \mathbf{J}/(GM_\odot) - \hat{r}_b = -\hat{r}_b$. Finally, determining the position of the comet as a function of time requires specifying the time that the comet passes through periapse, τ.

We call each perturber a "star," and write the velocity of the star $\mathbf{v}_p$. The mass of the star, m_p, will typically be about the same magnitude as $M_\odot$, the mass of the sun; both are very large compared to the mass of the comet, m_c. We focus this analysis on the regime where the path of the star is unaffected by the gravity of the Sun, or $GM_\odot/(bv_p^2) \ll 1$. Then the position of the perturber as a function of time is given by $\mathbf{r}_p(t) = \mathbf{b} + \mathbf{v}_p(t - t_0)$, where $\mathbf{b}$ describes the closest position of the star relative to the sun and t_0 is the time at which the star reaches this position.

We consider, at first, encounters between the star and the sun that occur with $b \gg 2a$, such that the perturbation to the sun-comet system can be treated in the tidal limit. We will show that these interactions are important for setting the angular momentum distribution when it is near zero. In section 4 we derive the evolution of the angular momentum as it evolves under all types of encounters including $b \leq a$.

In this case the tidal acceleration as a function of time is given by:

$$\mathbf{a}_T(t') = Gm_p r_b(t') \left[\frac{\hat{v}_p(\hat{r}_b \cdot \hat{v}_p) - \hat{r}_b}{(b^2 + (v_p t')^2)^{3/2}} - 3\frac{(\mathbf{b} + \mathbf{v}_p t)(\mathbf{b} \cdot \hat{r}_b)}{(b^2 + (v_p t')^2)^{5/2}} \right], \tag{1}$$

where we have translated the time coordinate by t_0 to simplify the expression.

The acceleration caused by each passing star affects the shape of the comet's orbit. Since the angular momentum is initially zero, the small impulses have a large relative effect on $\mathbf{J}$. In contrast, single perturbations to $\mathbf{e}$ and a are always small compared to their initial magnitudes. The periapse of the comet, which is important for determining the influence of the planets on the comet, is related to the angular momentum, $J = \sqrt{2GM_\odot q}$. For these reasons, we focus on understanding the effects of the stellar perturbations on the angular momentum vector.

To find the total change in angular momentum for one stellar passage, we integrate the acceleration over the motion of the star and of the comet: $\Delta\mathbf{J} = \int \mathbf{r}_b(t') \times \mathbf{a}_T(t') dt'$. There are two limiting cases where we can evaluate this integral to find a closed form solution. The first is the impulsive regime, where $b/v_p \ll T_{\rm orb}$. The comet spends most of its time with $r_b \sim a$; however, for rare interactions that occur when $r_b(t) \ll a$, impulsiveness requires $b/v_p \ll r_b(t)/v_b(t)$. We treat the comet as stationary over the duration of an impulsive perturbation: $r_b(t') = r_b(t_0)$, and find the change in angular momentum to be:

$$\Delta\mathbf{J}(t_0) = \frac{2Gm_p r_b(t_0)^2}{v_p b^2} \left[(\hat{r}_b \times \hat{v}_p)(\hat{r}_b \cdot \hat{v}_p) - 2(\hat{r}_b \times \hat{b})(\hat{r}_b \cdot \hat{b}) \right]. \tag{2}$$

The other simplifying case is a very non-impulsive encounter ($b/v_p \gg T_{\rm orb}$). When each orbit is very short relative to the timescale of the perturbation, the acceleration at each point along the perturber's path is experienced by the entire span of the comet's orbit. The disparate timescales in this regime allows the integral over the motion of the comet to be separated from the integral over the path of the star. The result is a $\Delta\mathbf{J}$ that is independent of t_0 and τ:

$$\Delta\mathbf{J} = \frac{5}{2}\frac{Gm_p}{v_p}\left(\frac{a}{b}\right)^2 \left[(\hat{r}_b \times \hat{v}_p)(\hat{r}_b \cdot \hat{v}_p) - 2(\hat{r}_b \times \hat{b})(\hat{r}_b \cdot \hat{b}) \right]. \tag{3}$$

This result also follows from replacing $r_b(t_0)^2$ in Equation 2 with its time averaged value, $\langle r_b^2 \rangle = (5/2)a^2$.

3. LÉVY FLIGHT BEHAVIOR

Successive perturbations cause the angular momentum delivered to the comet to accumulate. Individual perturbations add to the existing angular momentum vectorially: $\mathbf{J}_{\rm new} = \mathbf{r}_b \times (\mathbf{v}_b + \mathbf{\Delta}v) = \mathbf{J} + \Delta\mathbf{J}$. Holding $\hat{r}_b$ constant restricts the angular momentum vector to a plane. We accordingly treat $\mathbf{J}$ as a two-dimensional vector throughout this work. Since the perturbations by passing stars occur randomly, we employ the same statistical approach as CS08. We study the evolution of $\mathbf{J}$ by deriving a distribution function, $f(\mathbf{J}, t)$, that specifies the probability that the comet will have an angular momentum within the region $d^2\mathbf{J}$ around $\mathbf{J}$ at time t. If we assume that the perturbations occur isotropically, there is no preferred direction for the accumulated angular momentum of the comet. We then expect that $f(\mathbf{J}, t) = f(J, t)$. The probability of finding the comet's angular momentum with a magnitude between J and dJ in any direction is $2\pi f(J, t) J dJ$. We relax the assumptions of isotropy in Section 4.

We express the probability density function (PDF) for single perturbations as a frequency per unit angular momentum, $\mathcal{R}(J')$. This function describes the probability per unit time that the comet receives a perturbation with a magnitude between J' and $J' + dJ'$. Given the properties of the ensemble of perturbing stars, we compute the frequency with the following expression:

$$\mathcal{R}(J') = \int \delta(|\Delta\mathbf{J}(\mathbf{v}_p, \mathbf{b}, t_0, m_p)| - J') \mathcal{F}(\mathbf{v}_p, m_p) v_p \delta(\mathbf{b} \cdot \hat{v}_p) d^3\mathbf{b} d^3\mathbf{v}_p dm_p d(t_0/T_{\rm orb}). \tag{4}$$

where the function $\mathcal{F}(\mathbf{v}_p, m_p)$ is the combined phase space density of perturbers in $\mathbf{v}_p$ and m_p, normalized such that the total mass density of perturbers in real space is $\rho = \int m_p \mathcal{F}(\mathbf{v}_p, m_p) d^3\mathbf{v}_p dm_p$. This equation is analogous to Equation 9 of CS08, and is a precise formulation of the idea that the frequency at which the comet is perturbed by an amount of order J' is calculated by $J'\mathcal{R}(J') \sim nvb^2$, where n is the number density of perturbers, v is the velocity at which they encounter the sun-comet system, and b^2 is the cross-sectional area for such an encounter. In words, Equation 4 integrates over the entire parameter space of the encounter geometry ($\mathbf{v}_p, \mathbf{b}, t_0$, and m_p), weights the integral by the probability density of each parameter, and uses the delta function of $|\Delta J(\mathbf{v}_p, \mathbf{b}, t_0, m_p)|$ to select those geometries that produce a perturbation of size J'.

The frequency of perturbations is linked to the distribution function through a Boltzmann equation:

$$\frac{\partial f(J,t)}{\partial t} = \int p(\mathbf{J}')[f(|\mathbf{J}' + \mathbf{J}|) - f(J)] d^2\mathbf{J}'. \tag{5}$$

As in CS08, the function $p(\mathbf{J}')$ describes the frequency per unit angular momentum space ($d^2\mathbf{J}'$) at which a comet with angular momentum $\mathbf{J}$ is perturbed to $\mathbf{J} + \mathbf{J}'$; this is the PDF of $\mathbf{J}'$. We expect this frequency to depend only on the magnitude of the perturbation and not the direction, $p(\mathbf{J}') = p(J')$, for isotropic perturbers. It is related to $\mathcal{R}(J')$ by integrating $p(J')$ over the angular component of $\mathbf{J}'$, $\mathcal{R}(J') = 2\pi J' p(J')$.

We assume that the stellar perturbers have only one mass, m_p, and one velocity, v_p, that can point in any direction. The calculation of $p(J')$ then proceeds similarly to the calculation presented in CS08. Since the angular momentum excited by a perturber is proportional to m_p, v_p, and b in all the same ways as the excitation of eccentricity in a nearly circular binary, $J' \propto m_p/(v_p b^2)$ from Equations 2 and 3, it follows that $J'\mathcal{R}(J') \propto J'^{-1}$, and $p(J') \propto J'^{-3}$.

The full calculation of $p(J')$ requires choosing the correct expression for $\Delta\mathbf{J}$ given the timescale of the encounters. In the extremely non-impulsive regime (Equation 3), $\Delta\mathbf{J}$ is averaged over $r_b(t)$ before being used in Equation 4. For the impulsive case, $\Delta\mathbf{J}(t_0)$ retains its dependence on the position of the comet, but the subsequent integral over t_0 in Equation 4 averages the contribution of perturbers from all possible r_b. Ultimately we arrive at the same $p(J')$ for both non-impulsive and very impulsive perturbations:

$$p(J') = 0.74 G\rho a^2 \frac{1}{J'^3}, \tag{6}$$

where $\rho = nm_p$, the volumetric mass density of the perturbers in space. As noted in CS08, this form of $p(J')$ reveals that the angular momentum of the comet follows a Lévy flight (Shlesinger et al. 1995). The distribution function is then:

$$f(J,t) = \frac{1}{2\pi J_c^2(t)} (1 + (J/J_c(t))^2)^{-3/2}. \tag{7}$$

This function is self-similar, meaning that it always has the same shape centered around a characteristic angular momentum scale, $J_c(t)$, that changes with time. We have chosen the normalization such that $\int f(J,t) d^2\mathbf{J} = 1$ at all times. The characteristic angular momentum is near the median of the distribution, $J_{\rm median} = \sqrt{3} J_c(t)$. Since the probability of finding the comet with an angular momentum of order $J \gg J_c(t)$ falls off like the power law J^{-1}, the mean, variance, and all higher moments of the distribution are undefined. The mean only diverges logarithmically; if there is a maximum angular momentum $J_{\rm max}$, then $J_{\rm mean} = 2.3 J_c(t) \log_{10}(0.74 J_{\rm max}/J_c(t))$.

The time derivative of $J_c(t)$ is related to the perturbation frequency:

$$\dot{J}_c(t) = 4.66 G\rho a^2 \tag{8}$$

This equation is derived by substituting the solution for $f(J,t)$ (Equation 7) into the Boltzmann equation (Equation 5). Equation 8 determines $J_c(t)$ even if the parameters of the perturbing swarm (ρ) or the comet (a) are changing with time. During the formation of the Oort cloud, the semimajor axes of the comets evolve as the ice giants deliver orbital energy to them over many interactions. Additionally, a time-varying density of perturbers may be relevant if the Sun formed in a dense cluster (Fernandez 1997). The high eccentricity but high periapse orbit of Sedna may imply that the Sun was born in such an environment (Morbidelli & Levison 2004; Brasser et al. 2006; Kaib & Quinn 2008). A realistic statistical description of the formation of the Oort cloud must incorporate the evolution of ρ and a of the comets.

To provide the following simple numerical example, we assume a constant ρ and a. The angular momentum distribution function in this case grows linearly with time, $J_c(t) = 4.66 G\rho a^2 t$, for $J_c(t) \gg J_c(t=0)$. Using values relevant for the Oort cloud, we find

$$\frac{J_c(t)}{J_{\rm circ}} = 0.363 \left(\frac{\rho}{0.1 M_\odot {\rm pc}^{-3}}\right) \left(\frac{a}{10^4 {\rm AU}}\right)^{3/2} \left(\frac{t}{1 {\rm Gyr}}\right), \tag{9}$$

where we have scaled $J_c(t)$ by the angular momentum per unit mass of a circular orbit, $J_{\rm circ} = \sqrt{GM_\odot a}$, to make it dimensionless. Since our derivations neglect the non-radial motion of the comet's evolving orbit, our theory is only quantitatively correct for $J/J_{\rm circ} \ll 1$.

This mode of growth is qualitatively different from the typical diffusive random walk. The passing stars cause a spectrum of perturbations that occur with frequencies inversely proportional to their size ($J'\mathcal{R}(J') \propto J'^{-1}$). This power law is such that the smallest kicks cannot accumulate fast enough to affect the distribution function. For example, perturbations of about the same size accumulate as a normal diffusive random walk, $\delta J \propto \sqrt{t/t_{\rm small}} J'_{\rm small}$. In that same time, however, the comet receives, on average, a single perturbation of size $\delta J \approx J'_{\rm big} \propto (t/t_{\rm small}) J'_{\rm small}$. Thus the overall growth of the angular momentum is due to the few largest perturbations that occur over a time t.

The distribution in angular momentum (Equation 7) can be converted to a distribution for the comet's periapse distance, q, using the relation for nearly radial orbits, $J = \sqrt{2GM_\odot q}$:

$$f(q,t) = \frac{1}{2q_c(t)}(1 + q/q_c(t))^{-3/2}, \tag{10}$$

where $q_c(t)$ is the characteristic periapse associated with $J_c(t)$. We have chosen a normalization such that $\int f(q,t)dq = 1$. Since $J_c(t) \propto t$, the typical periapse distance grows as t^2; the timescale for a significant change in periapse then depends on the comet's current q.

These derivations of the distribution of a comet's angular momentum assumed the swarm of perturbers had a single individual mass and single velocity. If there are other massive perturbers with $m_p > M_\odot$, such as giant molecular clouds, Equations 7 and 9 describe the distribution when ρ includes all of the perturbers: $\rho = \sum n_i m_{p,i}$, where n_i and $m_{p,i}$ are the volumetric number density and masses of the ith group of perturbers. A mass spectrum that extends significantly below the mass of the Sun also affects the probability distribution of the perturbations. In the generalized case, the slope of the perturbation spectrum sets the high J power law of the distribution function. As long as the exponent of $J'\mathcal{R}(J')$ is between 0 and -2, the angular momentum follows a Lévy flight (Shlesinger et al. 1995). For the precise details of deriving $p(J')$ and $f(J',t)$ given a general mass distribution, we refer the reader to CS08.

4. CONNECTION TO GALACTIC TIDES

In deriving the model presented in Section 3, we have assumed that the perturbing stars are distributed isotropically in $\hat{v}_p$ and uniformly in impact parameter. We expect the angular momentum distribution in that scenario to be axisymmetric. Field stars, which are confined to a disk with a height much less than its radial dimension, do not have these simplifying properties. This section uses a toy model to show how an anisotropy in the angular momentum distribution arises from the spatial inhomogeneity of the perturbing stars, and how this is related to the angular momentum distribution discussed in section 3.

Heisler & Tremaine (1986) investigated the effects of the large scale potential arising from the Galactic disk. We reproduce their derivation of such a torque given a simple planar model of the mass distribution. We approximate the disk as a stack of infinitely thin, infinitely large sheets of mass. Gauss' law shows that the sheets above and below both the sun and the comet produce no net acceleration on the system. The sheets that pass in between the sun and comet however, produce a mean torque given by:

$$\dot{\mathbf{J}} = -2\pi G\rho(\mathbf{r}_b \cdot \hat{z})(\mathbf{r}_b \times \hat{z}), \tag{11}$$

where ρ is the local volumetric mass density in perturbers, and $\hat{z}$ is the unit vector normal to the disk plane. To an order of magnitude, this torque is the same as our Equation 8, although it is of a completely different nature. Equation 11 describes a smooth torque in a fixed direction, while Equation 8 is the typical value of a stochastic variable drawn from an axisymmetric distribution with zero mean.

Heisler & Tremaine (1986) also performed numerical experiments to verify that on very long timescales, stellar scattering indeed produces a mean growth on top of the stochastic evolution. The importance of the Galactic tides has been appreciated in subsequent studies of Oort cloud dynamics (Duncan et al. 1987; Heisler 1990; Dones et al. 2004; Rickman et al. 2008), although the relationship between the stellar encounters and the tidal torques is rarely addressed. Tidal torques are usually treated as separate from the effects of stellar encounters, even though the torque is provided by the same stars that cause the stochastic evolution. By adapting our formalism to reflect a planar distribution of perturbers, we reproduce the effects of the Galactic tides, and in doing so find the distribution function that accounts for both modes of angular momentum growth.

We follow the example of the numerical experiments of Heisler & Tremaine (1986) and approximate the Galaxy locally as a uniform disk of material, with a height much smaller than the scale of the other two dimensions. To create the planar symmetry in the model of stellar encounters, the velocities of the perturbers are restricted to a single direction. While this is not a realistic representation of the directional distribution of field star velocities, it is a simple model to explore and provides a clear example with which to examine the effects of a velocity asymmetry. With $\hat{v}_p$ fixed, the impact parameter $\mathbf{b}$ is confined to a plane, the aspect ratio of which has a much smaller height than width. Both of these properties, a single direction for $\hat{v}_p$ and a non-unity aspect ratio, introduce asymmetries in the distribution function of the comet's angular momentum.

For isotropic perturbers, perturbations of any size J' occur with the same likelihood in all directions in the plane perpendicular to r_b. This ensures that the mean of $\mathbf{J}(t)$ is zero, even though the typical magnitude of the angular momentum increases linearly with time. The cross-section for an interaction in the tidal limit ($b \gg r_b$) scales as b^2, which fixes the power law of the single perturbation PDF. In the planar model, the cross-sectional area that contributes perturbations with small J' is less than b^2 for impact parameters larger than the disk height. The contributions of these

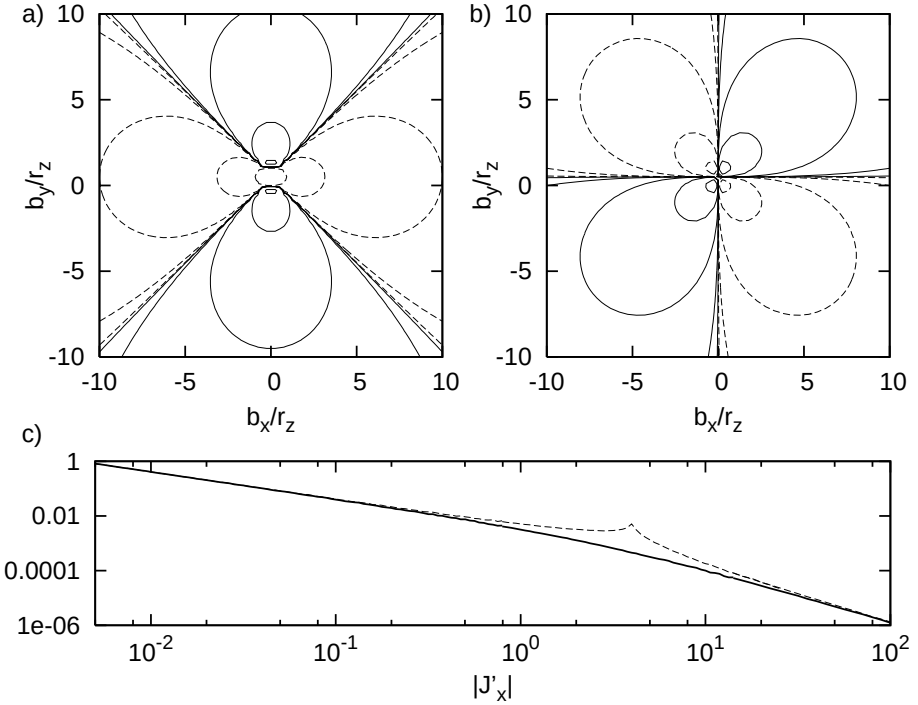

FIG. 1.— Contours of constant J' on the space of impact parameters $\mathbf{b}/(\mathbf{r}_b \cdot \hat{z})$ for positive and negative values of each component of the vector perturbation. The levels are spaced in multiples of ten from $J'/(2Gm_p/v_p) = \pm 10^{-4}$ to ± 1. Panel b, which shows the contours for the $\hat{y}$ direction, is symmetric with respect to positive and negative perturbations. The center of panel a shows an isolated region of negative $\hat{x}$ perturbations that causes an asymmetry in the distribution function. By randomly sampling this space of impact parameters we generate the PDF of the perturbations. The marginal PDF for positive and negative J'_x are plotted in panel c; the spike contains perturbations from the central region of panel a and is the source of the Galactic tidal torques on the comet.

regions to each component of $\mathbf{J}'$ depends on the angle between the comet and the disk plane so the axisymmetry is broken. However, these differences manifest only in the lowest J', and their effects on the distribution of accumulated angular momentum are always washed out by the larger perturbations from impact parameters less than the disk height.

Another asymmetry results from the impact parameters of $b \sim r_b$. For $b > r_b$, there is as much cross-sectional area contributing positively to each component as there is negatively. Impact parameters that pass between the sun and the comet, however, impart angular momentum in one direction of one component only, depending on the angle between $\hat{r}_b$ and $\hat{v}_p$. Not coincidentally, the mean torque found in the smooth distribution limit, Equation 11, is attributed to the disk of stars passing between the Sun and the comet.

We quantify the effect of this asymmetry by calculating the marginal probability density of each component of the angular momentum vector due to single interactions. Since we have lost the symmetry that admitted the simple analytic solutions, we employ a Monte-Carlo procedure. The position of the comet, which we hold fixed in this example, is $\mathbf{r}_b = \hat{y} + \hat{z}$, so the Sun-comet distance is $r_b = \sqrt{2}$. The perturber velocities are set to the $\hat{z}$ direction: $\hat{v}_p = -\hat{z}$. The possible impact parameters of the perturbers are then restricted to the $x - y$ plane. We randomly choose impact parameters such that they are uniformly distributed over the plane and calculate the $\mathbf{\Delta J}$ delivered to the comet. We assume the other parameters of the system are held constant (v_p and m_p), and to reduce the notation, we use units where $2Gm_p/v_p \equiv 1$. The angular momentum is confined to the plane perpendicular to $\mathbf{r}_b$, which in these coordinates is defined by the basis vectors $\hat{x}$ and $(\hat{y} - \hat{z})/\sqrt{2}$. For simplicity we discuss the x and y components of the perturbation, $\mathbf{\Delta J} \cdot \hat{x} = J'_x$ and $\mathbf{\Delta J} \cdot \hat{y} = J'_y$. In the z-direction, $\mathbf{\Delta J} \cdot \hat{z}$ is exactly the same as J'_y. The positive and negative values for J'_x and J'_y are binned separately; the resulting four histograms then describe the marginal PDF for each component.

Figure 1 illustrates the calculation of the single interaction PDF. Panels a and b show logarithmically spaced contours of constant J'_x and J'_y respectively in the plane of possible impact parameters, with the other parameters of the interaction fixed $(\mathbf{r}_b, \mathbf{v}_p, m_b)$. The impact parameter plotted is scaled by $\mathbf{r}_b \cdot \hat{z} = r_z = 1$. The solid contours correspond to positive perturbations and the dashed lines to negative ones. In panel b), the contours for $\pm J'_y$ exhibit an axisymmetric pattern; for each unit of area that contributes perturbations of a given magnitude greater than zero, there is an equivalent area where perturbations have the opposite sign. Thus the single interaction marginal PDF of perturbations in the $\hat{y}$ directions are identical and unchanged from the isotropic case: ${J'_y}^{-1}$ for the distant perturbations, $J'_y(b \gg r_b)$, and ${J'_y}^{-2}$ for the close encounters, $J'_y(b \ll r_b)$. There is no coherent accumulation of angular momentum in the $\hat{y}$ direction.

The contours of panel a), while symmetric at larger $\mathbf{b}$, are not symmetric in the center, where the perturbations only add angular momentum in the negative $\hat{x}$ direction. There is no equivalent area that delivers angular momentum

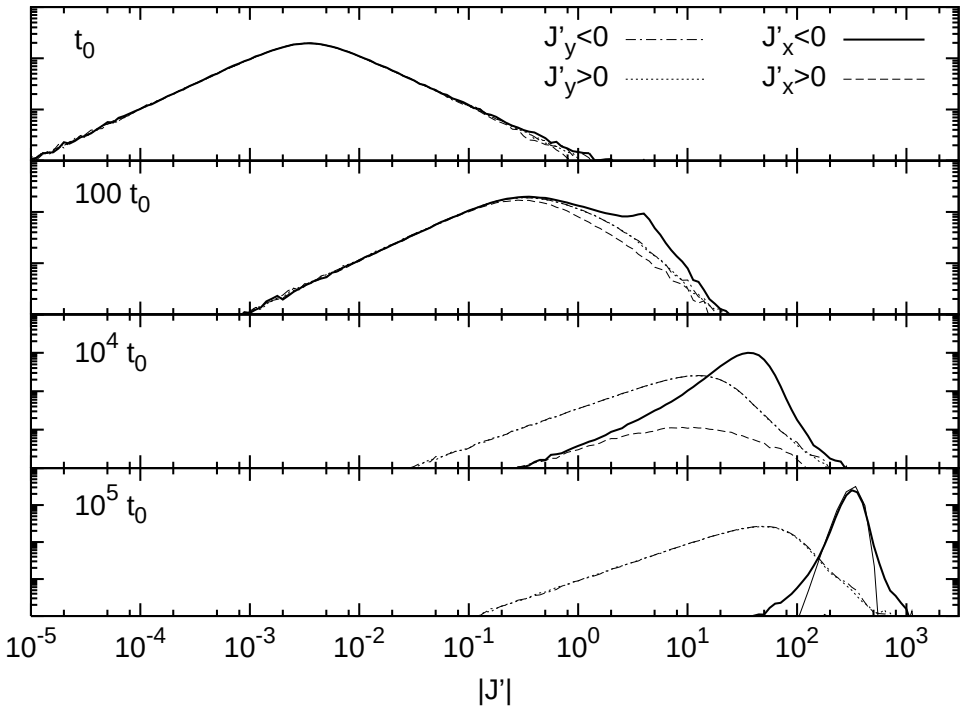

FIG. 2.— Marginal distribution functions of two components of the angular momentum as a function of time. The dotted and dot-dashed lines plot the marginal distribution, $dN/d(\log|J_y|)$, of the $\hat{y}$ component of the angular momentum $\mathbf{J}(t)$. The thick line is the distribution of the $\hat{x}$ component when it is negative, and the dashed line is the positive side. In the top two panels, the comet's angular momentum is best described by the Lévy flight behavior caused by stochastic stellar perturbations. In the bottom two, the coherent torque attributed to the Galactic tides dominates the evolution, causing a visibly asymmetric distribution. The thin line in the bottom panel is a Gaussian distribution with the mean given by the Galactic tidal torques and the variance given by the variance of the single interaction PDF multiplied by the number of encounters.

with the opposite sign. We plot the marginal PDF of J'_x, $|J'_x|\mathcal{R}(J'_x)$, in panel c) of Figure 1, where the solid line is for perturbations where $J'_x > 0$ and the dashed line is for $J'_x < 0$. The values along the ordinate represent the probability of perturbations with strength of order J'_x relative to the lowest value plotted. In the tidal and close encounter regimes, the two functions are identical. For J'_x of order unity, the contribution of the central region in panel a) is obvious. It is these interactions that give rise to the torque associated with the Galactic tides.

The marginal PDF of $\mathbf{J}'_x$ highlights the source of the Galactic tidal torque. However, it remains to describe how this manifests in the time-dependent distribution function of the comet's angular momentum. In Section 3, we used the Boltzmann equation (Equation 5) to relate the axisymmetric single perturbation PDF ($p(J')$) to the distribution of angular momentum ($f(\mathbf{J}(t))$). That derivation, however, depends on the simplifications afforded by the single power law form of $p(J')$. For the non-axisymmetric single perturbation PDF depicted in Figure 1, an analytic solution to the corresponding Boltzmann equation would be much more difficult to calculate.

Instead, we use a bootstrap technique to estimate the distribution function from a sample of single perturbations. The velocity of the perturbers, v_p, their number density, n, and the area sampled when generating the single interaction PDF, $\pi b^2_{\rm max}$, set the average time associated with each perturbation, $1/\tau = n\pi b^2_{\rm max} v_p$. The angular momentum at a time t is then the sum of t/τ single perturbations. By randomly choosing t/τ perturbations from the PDF and adding them vectorially, we generate a sample of angular momentum vectors that reflect the distribution function at that time t.

To accurately probe the evolution over many orders of magnitude, several single interaction PDFs with different $b_{\rm max}$ were used. Ignoring large impact parameters increases τ, or equivalently, samples the close encounters more often over a fixed number of perturbations. We verified that the distribution functions calculated with large τ (small $b_{\rm max}$) are not significantly affected by ignoring the frequent perturbations of smaller J'.

The marginal distribution functions at four different times are shown in Figure 2. Each histogram contains 10^6 bootstrapped $\mathbf{J}(t)$, generated from the sum of between 4 and 1000 single perturbations. The distribution of $J_y(t)$ is plotted in the dotted lines for $J_y(t) > 0$ and dash-dotted for $J_y(t) < 0$. For $J_x(t)$, the solid line represents the negative perturbations and the dashed line the positive ones.

The top panel shows the angular momentum distribution at early times, or equivalently, at low typical angular momenta. For reference, we denote this time t_0. Since the single interaction PDF for perturbations of this magnitude is axisymmetric, all four functions are identical. The excess of perturbations to negative J'_x is not visible as the likelihood for those encounters is too low to be sampled in the 10^6 vectors generated for the plot.

The second panel depicts the four distribution functions 100 times later than the time of the top panel. Again both functions show a similar shape, and the typical value for all four has grown linearly with time as predicted by

Equation 8. The trajectories passing between the sun and the comet have been sampled in a small fraction of the generated $\mathbf{J}(t)$, and the contribution from the spike of Figure 1c is apparent. Additionally the normalization of the positive distribution of $J_x(t)$ has fallen to reflect the breaking of the symmetry around $J_x = 0$. The distributions in the first and second panel can be said to be dominated by the influence of the stellar perturbations, and are not strongly affected by Galactic tides. Although the mean of the distribution is always set by the tides (see Equation 11), here this value of angular momentum is only realized after rare but strong interactions. The most likely angular momentum vectors, at early times, are distributed axisymmetrically around the origin.

In the third panel the non-axisymmetric growth is manifest. Due to the higher slope of the single encounter PDF, the distribution of the y component of the angular momentum has begun to grow only as $t^{1/2}$; the accumulations of kicks from all of the impact parameters smaller than r_b contribute to the shape of this distribution. Unfortunately a PDF of this slope does not admit a self-similar distribution function; asymptotically, the distribution approaches a Gaussian logarithmically over time (Shlesinger et al. 1995).

The perturbers passing between the sun and the comet deliver angular momentum in the $-\hat{x}$ direction coherently and thus the typical $-J_x(t)$ continues to increase linearly in time. The normalization of the histogram for positive $J_x(t)$ has decreased substantially, which is another indicator that the total distribution of $J_x(t)$ is no longer centered on the origin. In the fourth panel, only 10 times later than the third, the marginal distribution function for $J_x(t)$ is entirely dominated by the accumulated effects of non-canceled encounters. There are no values of $J_x(t) > 0$ in the sample at this time. Again, the distribution function does not admit an analytic form. For reference, we plot a Gaussian distribution with the mean described by Equation 11, and the variance expected given the single encounter PDF, $\sigma^2 = \sigma^2_{\rm PDF} t$. The distribution function only approaches this approximated shape logarithmically in time.

Figure 2 reveals the nature of the coherent torque by Galactic tides as merely the long term effects of anisotropic stellar encounters. It is only a matter of principle what to call the interactions of the comets with field stars. To determine the relevant behavior, one must specify which impact parameters are the most important for the behavior of the comet. On shorter timescales, or for smaller angular momenta, the distant perturbations create the axisymmetric distribution function associated with stochastic stellar encounters. Over timescales long enough that many trajectories have sampled the region between the Sun and comet, the system is best characterized as evolving under the Galactic tides.

As a physical example, we again examine the formation of the Oort cloud, where a proto-comet must gain enough angular momentum to raise its periapse q by Δq to avoid perturbations from the planets. The influence of the planets falls off rapidly with increasing q, so a reasonable value for $\Delta q/q$ is on the order of 10% (Duncan et al. 1987). The distant stellar encounters will be responsible for building the Oort cloud if a single interaction at an impact parameter $b \sim a$ can provide enough angular momentum to increase the periapse. If these single encounters are too weak, the coherent growth due to Galactic tides is required. We find the following inequality for when the mean tidal growth, rather than stochastic evolution, dominates:

$$\left(\frac{\Delta q}{q}\right)\left(\frac{M_\odot}{m_p}\right)\left(\frac{v_p}{v_q}\right) \gg 1, \tag{12}$$

where $v_q = (G m_\odot / q)^{1/2}$ is the local rotational velocity at periapse. At the semimajor axis of Jupiter, this velocity is about 15 km s^{-1}, and near Neptune it is about 5 km s^{-1}. Typical velocity dispersions of stars in the solar neighborhood are $15 - 40$ km s^{-1} (Binney & Tremaine 1987). Then in the inner solar system, the tidal torque is less important than the stellar encounters for freeing the comets from planetary perturbations. In the outer solar system, the left hand side of Equation 12 is close to unity, meaning the stellar encounters and the tidal torque play a comparable role.

Our new understanding of the relationship between stellar encounters and tides presents a clearer picture of the most appropriate way to model the excitation of angular momentum in an Oort cloud comet. If the prescription for stellar encounters includes the planar symmetry of the stars, then no extra torque is required to represent the Galactic tides. If the stellar encounter model has an isotropic velocity distribution, then an extra term representing the torque should be included, but only at late enough times that encounters passing between the sun and the comet are common.

5. CONCLUSIONS

In this work we have shown that the angular momentum delivered to nearly radial comets by passing stars follows a Lévy flight. From the properties of a single scattering between the comet and the star, we derive the distribution function of the angular momentum of the comet as a function of time. Our calculations agree with the estimates made in earlier work on Oort cloud formation, that stellar perturbations can raise the periapses of comets significantly in only several hundred Myrs. A careful examination of the scattering process for an anisotropic velocity distribution reveals the presence of the coherent angular momentum growth that is usually attributed to the large scale potential of the Galaxy. The effects of stellar encounters and the Galactic tidal torques then cannot be treated as two distinct processes. On shorter timescales the distribution function of the comet is unaffected by the tidal torque; on long timescales the distribution is entirely dominated by it. Since the presence of the tidal torque depends on the perturber velocity distribution, simulations of cometary evolution that include stellar encounters must be careful not to double-count the Galactic tides by either including an explicit torque or enforcing a planar symmetry, but not both.

These results provide a formal understanding of the effects of stellar encounters on nearly radial comets, but it is only the first step towards a complete statistical picture of the formation of the Oort cloud. The shape of the distribution function of the angular momentum at early times will not be entirely isotropic due to the triaxial velocity distribution

of field stars; however, this anisotropy will be overwhelmed at the current epoch by effects of the Galactic tidal torque. The effects of the stellar perturbations must be convolved with the diffusion of the comets' semimajor axes caused by planetary perturbations. This type of diffusion is not without complications, as orbital resonances between the comet and the planet must be accounted for to produce accurate diffusion coefficients (Malyshkin & Tremaine 1999; Pan & Sari 2004). Additionally, the diffusion of the semimajor axis for a comet whose orbit crosses that of a planet has been shown to exhibit properties of a Lévy flight (Zhou et al. 2002).

We thank the Institute for Advanced Study for their hospitality while some of this work was completed. R.S. is a Packard Fellow. This work was partially supported by the ERC.

REFERENCES

Binney, J., & Tremaine, S. 1987, Galactic dynamics (Princeton, NJ, Princeton University Press, 747 p.)
Brasser, R., Duncan, M. J., & Levison, H. F. 2006, Icarus, 184, 59
Collins, B. F., & Sari, R. 2006, AJ, 132, 1316
—. 2008, AJ, 136, 2552
Collins, B. F., Schlichting, H. E., & Sari, R. 2007, AJ, 133, 2389
Dones, L., Weissman, P. R., Levison, H. F., & Duncan, M. J. 2004, Oort cloud formation and dynamics (Comets II), 153–174
Duncan, M., Quinn, T., & Tremaine, S. 1987, AJ, 94, 1330
Fernandez, J. A. 1997, Icarus, 129, 106
Heisler, J. 1990, Icarus, 88, 104
Heisler, J., & Tremaine, S. 1986, Icarus, 65, 13
Kaib, N. A., & Quinn, T. 2008, Icarus, 197, 221
Malyshkin, L., & Tremaine, S. 1999, Icarus, 141, 341
Morbidelli, A., & Levison, H. F. 2004, AJ, 128, 2564
Oort, J. H. 1950, Bull. Astron. Inst. Netherlands, 11, 91
Pan, M., & Sari, R. 2004, AJ, 128, 1418
Rickman, H., Fouchard, M., Froeschlé, C., & Valsecchi, G. B. 2008, Celestial Mechanics and Dynamical Astronomy, 102, 111
Shlesinger, M. F., Zaslavsky, G. M., & Frisch, U. e. 1995, Levy Flights and Related Topics in Physics (New York: Springer-Verlag)
Zhou, J.-L., Sun, Y.-S., & Zhou, L.-Y. 2002, Celestial Mechanics and Dynamical Astronomy, 84, 409